

Alignment and Precession of a Black Hole with a Warped Accretion Disc

Rebecca G. Martin, J. E. Pringle and Christopher A. Tout

University of Cambridge, Institute of Astronomy, The Observatories, Madingley Road, Cambridge CB3 0HA

ABSTRACT

We consider the shape of an accretion disc whose outer regions are misaligned with the spin axis of a central black hole and calculate the steady state form of the warped disc in the case where the viscosity and surface densities are power laws in the distance from the central black hole. We discuss the shape of the resulting disc in both the frame of the black hole and that of the outer disc. We note that some parts of the disc and also any companion star maybe shadowed from the central regions by the warp. We compute the torque on the black hole caused by the Lense-Thirring precession and hence compute the alignment and precession timescales. We generalise the case with viscosity and hence surface density independent of radius to more realistic density distributions for which the surface density is a decreasing function of radius. We find that the alignment timescale does not change greatly but the precession timescale is more sensitive. We also determine the effect on this timescale if we truncate the disc. For a given truncation radius, the the timescales are less affected for more sharply falling density distributions.

Key words: accretion, accretion discs - X-rays: binaries - galaxies: active - galaxies: jets - quasars: general

1 INTRODUCTION

Observations indicate that accretion discs around black holes can be warped. Warped discs have been observed in active galactic nuclei (AGN) by water maser observations in NGC 4258 (Herrnstein, Greenhill & Moran 1996) and in the Circinus galaxy (Greenhill et al. 2003). A warped inner accretion disc might explain why radio jets from AGN are not perpendicular to the plane of the Galactic disc (Kinney et al. 2000; Schmitt et al. 2002).

The two X-ray binaries GRO J 1655-40 and SAX J1819-2525 have also been observed to have jets misaligned with their orbital planes. For example, GRO J 1655-40 appears to have a binary orbit at 70° (Greene, Bailyn & Orosz 2001) and jet inclination at 85° (Hjellming & Rupen 1995). This implies that there is a misalignment of at least 15° between the inclination of the black hole and the outer parts of the accretion disc.

We consider a system with an accretion disc around a spinning black hole. The black hole spin is misaligned with the outer parts of the disc which we assume to be fixed by the plane of a binary companion. Lense-Thirring precession drives a warp in the disc which reaches a steady state when the inner parts are aligned with the black hole by the Bardeen & Petterson (1975) effect.

Scheuer & Feiler (1996) calculated the shape of the

steady disc and the timescale for the black hole to align on the assumption that the warping is gradual and that the viscosities and the surface density of the disc are independent of radius. Because in their analysis the orientation of the outer disc is fixed, the torque between the disc and the hole makes the black hole precess and makes its spin align with that of the disc (King et al. 2005). Scheuer & Feiler (1996) find that the alignment timescale and precession timescale are about the same in this case and this has been illustrated with numerical simulations by Lodato & Pringle (2006). However, in more realistic discs the surface density is a decreasing function of radius. For idealised discs in which in which shear viscosity ν_1 varies as a power law, $\nu_1 \propto R^\beta$, in radius R the steady state surface density Σ obeys $\Sigma \propto R^{-\beta}$ because $\nu_1 \Sigma$ tends to a constant far from the inner edge (Pringle 1981). Typically the power β lies in the range $0 \leq \beta \leq 2$.

Natarajan & Armitage (1999) discuss how the alignment timescale depends on β and suggest on dimensional grounds that the timescale increases by about a factor of 10 as β changes from 0 to 1.5. We compute the shape of the disc but our analysis differs from that of Natarajan & Armitage (1999) in that we compute how the precession and alignment timescales vary with the density distribution (β) when the warp radius and the accretion rate are fixed. We find that the alignment timescale does not vary strongly with β but that the precession timescale is more sensitive..

2 STEADY STATE SOLUTION

Our analysis follows that of Scheuer & Feiler (1996). We consider the disc to be made up of annuli of width dR and mass $2\pi\Sigma R dR$ at radius R from the central star of mass M with surface density $\Sigma(R, t)$ at time t and with angular momentum $\mathbf{L} = (GMR)^{1/2}\Sigma\mathbf{l} = L\mathbf{l}$. The unit vector describing the direction of the angular momentum of a disc annulus is given by $\mathbf{l} = (l_x, l_y, l_z)$ with $|\mathbf{l}| = 1$.

Like Scheuer & Feiler (1996) we derive a solution for the steady state disc profile described by $W = l_x + il_y$. We use equation (2.8) of Pringle (1992) setting $\partial\mathbf{L}/\partial t = 0$ and adding a term to describe the Lense-Thirring precession to give

$$0 = \frac{1}{R} \frac{\partial}{\partial R} \left[\left(\frac{3R}{L} \frac{\partial}{\partial R} (\nu_1 L) - \frac{3}{2} \nu_1 \right) L + \frac{1}{2} \nu_2 R L \frac{\partial \mathbf{l}}{\partial R} \right] + \frac{\boldsymbol{\omega}_{\mathbf{p}} \times \mathbf{L}}{R^3}. \quad (1)$$

There are two viscosities, ν_1 corresponds to the azimuthal shear (the viscosity normally associated with accretion discs) and ν_2 corresponds to the vertical shear in the disc which smoothes out the twist. The second viscosity acts when the disc is non-planar. The Lense-Thirring precession is given by

$$\boldsymbol{\omega}_{\mathbf{p}} = \frac{2G\mathbf{J}}{c^2}, \quad (2)$$

(Kumar & Pringle 1985) where the angular momentum of the black hole $\mathbf{J} = J\mathbf{j}$ with $\mathbf{j} = (j_x, j_y, j_z)$ and $|\mathbf{j}| = 1$ can be expressed in terms of the dimensionless spin parameter a such that

$$J = acM \left(\frac{GM}{c^2} \right). \quad (3)$$

We take both viscosities to have power law form so that

$$\nu_1 = \nu_{10} \left(\frac{R}{R_0} \right)^\beta \quad \text{and} \quad \nu_2 = \nu_{20} \left(\frac{R}{R_0} \right)^\gamma, \quad (4)$$

where ν_{10} , ν_{20} , β and γ are all constants and R_0 is some fixed radius. The surface density is

$$\Sigma = \Sigma_0 \left(\frac{R}{R_0} \right)^{-\beta}. \quad (5)$$

We take the scalar product of equation (1) with \mathbf{l} and find

$$0 = \frac{1}{R} \frac{\partial}{\partial R} \left[3R \frac{\partial}{\partial R} (\nu_1 L) - \frac{3}{2} \nu_1 L \right] \quad (6)$$

because $\mathbf{l} \cdot \partial\mathbf{l}/\partial R = 0$ when $|\mathbf{l}| = 1$. We assume the warp is gradual enough that we can neglect the non-linear term $\mathbf{l} \cdot \partial^2 \mathbf{l} / \partial R^2 = -|\partial\mathbf{l}/\partial R|^2$. We consider the effects of neglecting this term at the end of this section. This equation has the solution

$$\nu_1 L = C_0 R^{1/2} + C_1 \quad (7)$$

where C_0 and C_1 are constants. We set $L = 0$ at $R = 0$ and $L = (GMR)^{1/2}\Sigma$ so $C_1 = 0$ and

$$L = (GMR)^{1/2}\Sigma_0 \left(\frac{R}{R_0} \right)^{-\beta} \quad (8)$$

in the steady state as in the flat case.

Substituting equation (8) into equation (1) we find

$$-\frac{\boldsymbol{\omega}_{\mathbf{p}} \times \mathbf{l}}{R^2} L = \frac{\partial}{\partial R} \left[\frac{1}{2} R \nu_2 L \frac{\partial \mathbf{l}}{\partial R} \right]. \quad (9)$$

We work in the frame of the black hole where $\mathbf{J}/J = (0, 0, 1)$ so that $\boldsymbol{\omega}_{\mathbf{p}} = (0, 0, \omega_{\mathbf{p}})$ and $\boldsymbol{\omega}_{\mathbf{p}} \times \mathbf{l} = (-\omega_{\mathbf{p}} l_y, \omega_{\mathbf{p}} l_x, 0)$.

We add the x -component of equation (9) to i times the y -component, where $i = \sqrt{-1}$ and set $W = l_x + il_y$ to obtain

$$\kappa R^{-\frac{3}{2}-\beta} W = \frac{d}{dR} \left[R^{\gamma+\frac{3}{2}-\beta} \frac{dW}{dR} \right], \quad (10)$$

where

$$\kappa = -\frac{2i\omega_{\mathbf{p}}}{\nu_{20}} R_0^\gamma, \quad (11)$$

so that

$$\kappa^{\frac{1}{2}} = \pm(1-i) \left(\frac{\omega_{\mathbf{p}}}{\nu_{20}} \right)^{\frac{1}{2}} R_0^{\frac{\gamma}{2}}. \quad (12)$$

To simplify the analysis we let $\beta = \gamma$ so that the two viscosities obey the same power law and thus the ratio ν_1/ν_2 is independent of radius (c.f. Lodato & Pringle, 2007). Setting $x = R^{-\frac{1}{2}(1+\beta)}$ we find

$$\kappa x^{\frac{3+2\beta}{1+\beta}} W = \frac{(1+\beta)^2}{4} x^{\frac{3+\beta}{1+\beta}} \frac{d}{dx} \left(x^{\frac{\beta}{1+\beta}} \frac{dW}{dx} \right) \quad (13)$$

and setting $W(R) = R^{-\frac{1}{4}} V(R) = x^{\frac{1}{2(1+\beta)}} V(x)$ we obtain

$$x^2 \frac{d^2 V}{dx^2} + x \frac{dV}{dx} - \left(\frac{1}{(2(1+\beta))^2} + \left(\frac{2\kappa^{\frac{1}{2}}}{1+\beta} \right)^2 x^2 \right) V = 0. \quad (14)$$

This is a modified Bessel equation with solution

$$V = AI_{\frac{1}{2(1+\beta)}} \left(\frac{2}{1+\beta} \kappa^{\frac{1}{2}} x \right) + BK_{\frac{1}{2(1+\beta)}} \left(\frac{2}{1+\beta} \kappa^{\frac{1}{2}} x \right), \quad (15)$$

where $I_\nu(z)$ and $K_\nu(z)$ are the modified Bessel functions of the first and second kind respectively and A and B are constants to be determined.

We know that $W \rightarrow 0$ as $R \rightarrow 0$ because the inner disc is aligned with the spin of the black hole. Thus we take κ to have a positive real part and $A = 0$ so that the full solution is

$$W = B \left(\frac{R}{R_0} \right)^{-\frac{1}{4}} K_{\frac{1}{2(1+\beta)}} \left(\frac{2}{1+\beta} \kappa^{\frac{1}{2}} R^{-\frac{1}{2}(1+\beta)} \right). \quad (16)$$

In order to find B we need to consider what happens as $R \rightarrow \infty$. At large radius the disc tilt is taken to be fixed and thus we let $W \rightarrow W_\infty$ which is a constant. Thus as $R \rightarrow \infty$ we find

$$W \rightarrow \frac{BR_0^{\frac{1}{4}}}{2} \Gamma \left(\frac{1}{2(1+\beta)} \right) \left(\frac{\kappa^{\frac{1}{2}}}{1+\beta} \right)^{-\frac{1}{2(1+\beta)}} = W_\infty, \quad (17)$$

where we have made use of the relation

$$K_\nu(x) \sim \frac{\Gamma(\nu)}{2} \left(\frac{x}{2} \right)^{-\nu}, \quad (18)$$

as $x \rightarrow 0$. Rearranging we now find

$$B = \frac{2}{\Gamma \left(\frac{1}{2(1+\beta)} \right)} R_0^{-\frac{1}{4}} \left(\frac{\kappa^{\frac{1}{2}}}{1+\beta} \right)^{\frac{1}{2(1+\beta)}} W_\infty \quad (19)$$

and

$$W = W_\infty \frac{2}{\Gamma\left(\frac{1}{2(1+\beta)}\right)} \left(\frac{\kappa^{\frac{1}{2}}}{1+\beta}\right)^{\frac{1}{2(1+\beta)}} \times R^{-\frac{1}{4}} K_{\frac{1}{2(1+\beta)}} \left(\frac{2}{1+\beta} \kappa^{\frac{1}{2}} R^{-\frac{1}{2}(1+\beta)}\right). \quad (20)$$

We note that if $\beta = 0$ this reduces to

$$W = W_\infty \exp\left[-2(1-i) \left(\frac{\omega_p}{\nu_{20} R}\right)^{1/2}\right], \quad (21)$$

where we have made use of the identities $K_{1/2}(z) = e^{-z} \sqrt{\pi/(2z)}$ and $\Gamma(1/2) = \sqrt{\pi}$. This is the solution found by Scheuer & Feiler (1996).

The radius where the warp in the disc typically occurs, R_{warp} (Scheuer & Feiler 1996), can be found by balancing the terms on either side of equation (9). We find

$$R_{\text{warp}} = \left(\frac{2\omega_p}{\nu_{20}} R_0^\beta\right)^{1/(1+\beta)}. \quad (22)$$

In order to compare different power laws for viscosity in a reasonable way we want to keep ν_1 , ν_2 and Σ the same at R_{warp} where the torques are greatest. We therefore set

$$R_0 = R_{\text{warp}} = \frac{2\omega_p}{\nu_{20}} = \frac{4aG^2 M^2}{\nu_{20} c^3}. \quad (23)$$

and note that ν_{20} now corresponds to the value of ν_2 at the radius where the disc is warped. Equation (20) with $\kappa = -iR_{\text{warp}}^{1+\beta}$ becomes

$$W = \frac{2W_\infty}{\Gamma\left(\frac{1}{2(1+\beta)}\right)} \frac{(-i)^{\frac{1}{4(1+\beta)}}}{(1+\beta)^{\frac{1}{2(1+\beta)}}} \left(\frac{R_{\text{warp}}}{R}\right)^{1/4} \times K_{\frac{1}{2(1+\beta)}} \left(\frac{\sqrt{2}}{1+\beta} (1-i) \left(\frac{R}{R_{\text{warp}}}\right)^{-\frac{1+\beta}{2}}\right). \quad (24)$$

Note that we choose the negative root of $-i$ in equation (12) because we want the real part of the argument of the Bessel function to be positive. We note that in this solution we have a term of the form

$$K_\nu(e^{-i\pi/4} x) = e^{-i\nu\pi/2} (\ker_\nu(x) - i\text{kei}_\nu(x)), \quad (25)$$

where \ker_ν and kei_ν are Kelvin functions (Watson 1966).

The second order term, $|\partial \mathbf{l} / \partial R|^2$, which we choose to neglect, from equation (6) has a magnitude that is largest in the disc around R_{warp} but is negligible for small inclination angles. The largest error occurs when the outer disc is inclined at an angle of $\pi/2$ to the black hole. Then the relative magnitude of the neglected term is $0.049 \nu_{20} / \nu_{10}$ for $\beta = 0$. For $\beta = 3$ it grows to $0.093 \nu_{20} / \nu_{10}$. If $\nu_{20} < \nu_{10}$ the analysis is good for all inclinations of the outer disc. When this inclination is reduced to $\pi/6$ the relative magnitude of the neglected term has fallen to $0.023 \nu_{20} / \nu_{10}$ for $\beta = 3$ and $0.012 \nu_{20} / \nu_{10}$ for $\beta = 0$.

3 THE SHAPE OF THE DISC

In Figure 1 we plot the solution $W = l_x + il_y$ for various values of β as $l_x = \Re(W)$ against $l_y = \Im(W)$ with $W_\infty = 1$. Note that since the problem is a linear one, we may take

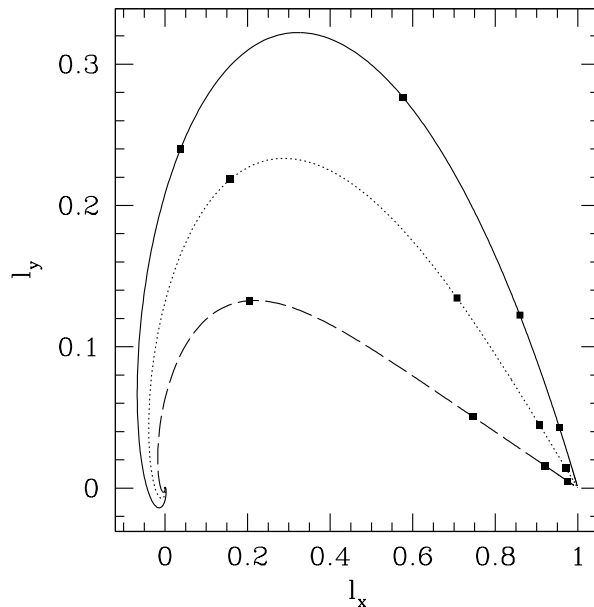


Figure 1. The steady state disc, l_y against l_x as R changes in the case with $W_\infty = 1$. The solid line has $\beta = 0$, the dotted line has $\beta = 3/4$ and the dashed line has $\beta = 3$. The lines begin at $R = 0$ at $l_x = l_y = 0$ and the dots on the curves are where $R = 1, 10, 100$ and $1000 R_{\text{warp}}$.

$W_\infty = 1$. In this plane, the completely flat, but inclined, disc would be a point at $W = 1$. As $R \rightarrow 0$ the disc becomes steadily more aligned with the black hole spin and $W \rightarrow 0$. The lower the value of β the less the disc is twisted. The lines begin at $R = 0$ at $l_x = l_y = 0$ and the dots on the curves are where $R/R_{\text{warp}} = 1, 10, 100$ and 1000 .

Kelvin functions are in effect combinations of the ordinary, oscillatory Bessel functions $J(x)$ and $Y(x)$ and the modified, non-oscillatory Bessel functions $I(x)$ and $K(x)$. Because of the nature of Kelvin functions and because, as $R \rightarrow 0$, the argument of the Bessel function tends to infinity, the solution $W(R)$ circles the origin an infinite number of times as $R \rightarrow 0$ while at the same time approaching the origin exponentially. Thus, as we approach the origin, the disc becomes very twisted, but very flat. This explains why, as remarked by Scheuer & Feiler (1996), numerical integration packages tend to fail for this problem.

The inclination of the disc relative to the black hole spin direction \hat{z} at radius R is

$$\theta(R) = \cos^{-1}(\hat{z} \cdot \mathbf{l}) = \cos^{-1}(l_z). \quad (26)$$

The solution for W is in the frame of the black hole where $\mathbf{J}/J = (0, 0, 1)$ and we have the disc angular momentum vector

$$\mathbf{l} = \left(\Re(W), \Im(W), \sqrt{1 - |W(R)|^2}\right). \quad (27)$$

Thus the inclination of the disc at radius R in this frame is

$$\theta_1(R) = \cos^{-1}\left(\sqrt{1 - |W(R)|^2}\right). \quad (28)$$

We can also find the disc inclination in the frame aligned with the outer disc regions. In this frame the inclination of the disc tends to zero as $R \rightarrow \infty$. This means as $R \rightarrow \infty$,

$\boldsymbol{l} \rightarrow (0, 0, 1)$. In this frame we take the angular momentum of the black hole, \boldsymbol{J}' , to have $j'_y = 0$ at $t = 0$ and so

$$\boldsymbol{J}' = J(-\sin \eta, 0, \cos \eta) \quad (29)$$

where η is the angle of inclination of the black hole spin to the outer disc axis and prime denotes quantities in the frame of the outer disc. The disc angular momentum direction vector becomes

$$\begin{aligned} l'_x &= l_x \cos \eta - l_z \sin \eta \\ &= \Re(W) \cos \eta - \sqrt{1 - |W|^2} \sin \eta \\ l'_z &= l_x \sin \eta + l_z \cos \eta \\ &= \Re(W) \sin \eta + \sqrt{1 - |W|^2} \cos \eta \\ l'_y &= l_y \end{aligned} \quad (30)$$

then

$$\theta_2(R) = \cos^{-1} \left(\Re(W) \sin \eta + \sqrt{1 - |W(R)|^2} \cos \eta \right). \quad (31)$$

If we transform back to the frame of the black hole we would need the transformation

$$\begin{aligned} l_x &= l'_x \cos \eta + l'_z \sin \eta \\ l_z &= -l'_x \sin \eta + l'_z \cos \eta \\ l_y &= l'_y \end{aligned} \quad (32)$$

and so we see that in the frame of the black hole as $R \rightarrow \infty$

$$\boldsymbol{l} \rightarrow (\sin \eta, 0, \cos \eta) \quad (33)$$

because $\boldsymbol{l}' = (0, 0, 1)$ and so we find

$$W_\infty = \sin \eta, \quad (34)$$

or more generally

$$W_\infty = -(j'_x + ij'_y). \quad (35)$$

3.1 Application to GRO J1655-40

As a real example we consider parameters relevant to the source GRO J1655-40 and take $\eta = 0.2618$ corresponding to an angle of 15° . We assume that the outer disc plane corresponds to that of the binary and that the inner disc is aligned with the spin of the hole which is parallel to the observed jet. In Figure 2 we plot the inclination in the frame of the black hole and in Figure 3 of the binary. The former shows that the warp steepens with increasing β . The latter shows that, in the frame of the binary, the inclination of the disc near $R = 0$ is higher than the inclination of the black hole. This hump, that is due to the precession of the disc around the hole, could shield the binary companion from the black hole radiation.

4 ALIGNMENT AND PRECESSION TIMESCALES

Having obtained the shape of the disc we are now able to calculate the mutual torque between it and the black hole. Because we assume the outer disc is fixed, this enables us to compute the timescale on which the black hole spin aligns with it and to compute the precession rate as it does so. We

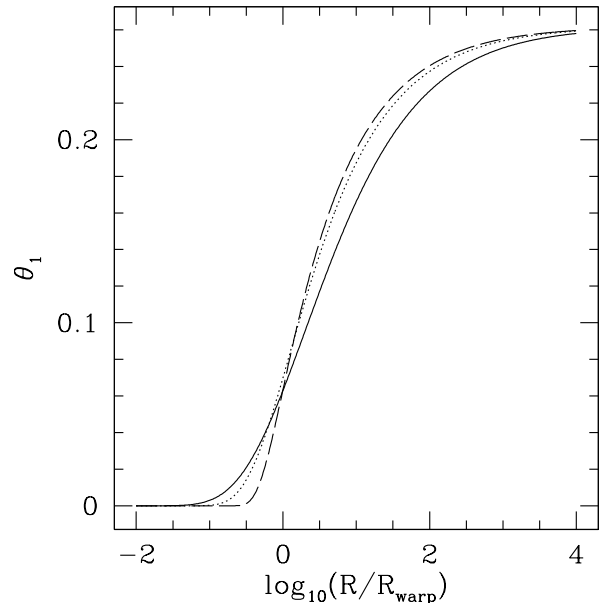


Figure 2. The inclination of the disc against R/R_{warp} in the frame of the black hole. The solid line has $\beta = 0$, the dotted line has $\beta = 3/4$ and the dashed line has $\beta = 3$.

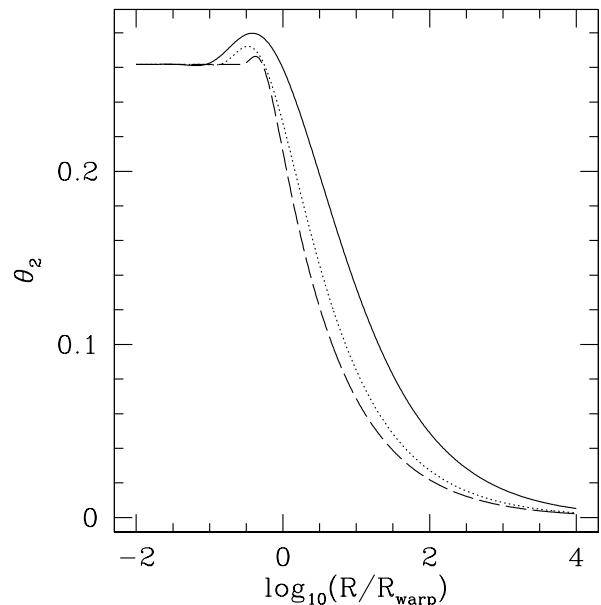


Figure 3. The inclination of the disc against R/R_{warp} in the frame of the binary. The solid line has $\beta = 0$, the dotted line has $\beta = 3/4$ and the dashed line has $\beta = 3$.

work in the frame of the black hole and the torque on the black hole is given by

$$-\frac{d\boldsymbol{J}}{dt} = \int_{\text{disc}} \frac{\boldsymbol{\omega}_p \times \boldsymbol{L}}{R^3} 2\pi R dR \quad (36)$$

$$= \int_{R_{\text{in}}}^{R_{\text{out}}} \omega_p(-l_y, l_x, 0) C_2 2\pi R^{-\frac{3}{2}-\beta} dR, \quad (37)$$

where R_{in} and R_{out} are the inner and outer edge of the disc and $C_2 = (GM)^{1/2} \Sigma_0 R_0^\beta$ is a constant. Adding the x -component to i times the y -component we obtain

$$\frac{d(J_x + iJ_y)}{dt} = -2\pi i \omega_p C_2 \int_{R_{\text{in}}}^{R_{\text{out}}} W R^{-\frac{3}{2}-\beta} dR \quad (38)$$

and using equation (16) to substitute for W we find

$$\begin{aligned} \frac{d(J_x + iJ_y)}{dt} = & -2\pi i \omega_p C_2 B R_0^{\frac{1}{4}} \int_{R_{\text{in}}}^{R_{\text{out}}} R^{-\frac{7}{4}-\beta} \\ & \times K_{\frac{1}{2(1+\beta)}} \left(\frac{2}{1+\beta} \kappa^{\frac{1}{2}} R^{-\frac{1}{2}(1+\beta)} \right) dR, \end{aligned} \quad (39)$$

where the constant B is defined by equation (19). We simplify the expression by taking dimensions out of the integral to obtain

$$\begin{aligned} \frac{d(J_x + iJ_y)}{dt} = & \frac{4\pi i \omega_p C_2}{1+\beta} B R_0^{\frac{1}{4}} \left(\frac{1+\beta}{2\kappa^{\frac{1}{2}}} \right)^{\frac{3+4\beta}{2(1+\beta)}} \\ & \times \int_{z_{\text{in}}}^{z_{\text{out}}} K_{\frac{1}{2(1+\beta)}}(z) z^{\frac{1+2\beta}{2(1+\beta)}} dz, \end{aligned} \quad (40)$$

where

$$z(R) = \frac{2}{1+\beta} \kappa^{\frac{1}{2}} R^{-\frac{1}{2}(1+\beta)}, \quad (41)$$

so that $z_{\text{in}} = z(R_{\text{in}})$ and $z_{\text{out}} = z(R_{\text{out}})$.

In Appendix 1 we show that

$$\begin{aligned} \int_0^{(1-i)\infty} K_c(z) z^d dz = & 2^{d-1} \Gamma \left(\frac{1}{2}(1-c+d) \right) \\ & \Gamma \left(\frac{1}{2}(1+c+d) \right) \end{aligned} \quad (42)$$

if $\Re(c-d) < 1$ and $\Re(c+d) > -1$. So with $c = 1/(2(1+\beta))$ and $d = (1+2\beta)/(2(1+\beta))$ this integral is valid for $\beta > -1/2$. We now have

$$\begin{aligned} \frac{d(J_x + iJ_y)}{dt} = & \frac{4\pi i \omega_p C_2}{1+\beta} B R_0^{\frac{1}{4}} \left(\frac{1+\beta}{2\kappa^{\frac{1}{2}}} \right)^{\frac{3+4\beta}{2(1+\beta)}} 2^{-\frac{1}{2(1+\beta)}} \\ & \times \Gamma \left(\frac{1+2\beta}{2(1+\beta)} \right) \end{aligned} \quad (43)$$

and using equation (19) to eliminate B we get

$$\begin{aligned} \frac{d(J_x + iJ_y)}{dt} = & \frac{2\pi i \omega_p C_2}{1+\beta} W_\infty \left(\frac{1+\beta}{\kappa^{\frac{1}{2}}} \right)^{\frac{1+2\beta}{1+\beta}} \\ & \times \frac{\Gamma \left(\frac{1+2\beta}{2(1+\beta)} \right)}{\Gamma \left(\frac{1}{2(1+\beta)} \right)}. \end{aligned} \quad (44)$$

In Section 3 we found that $W_\infty = -(j_x + ij_y)$. We define

$$\Gamma_\beta = \frac{\Gamma \left(\frac{1+2\beta}{2(1+\beta)} \right)}{\Gamma \left(\frac{1}{2(1+\beta)} \right)}, \quad (45)$$

so that

$$\frac{d(j_x + ij_y)}{j_x + ij_y} = \frac{2\pi i C_2 \omega_p}{1+\beta} \frac{1}{J} \left(\frac{1+\beta}{\kappa^{\frac{1}{2}}} \right)^{\frac{1+2\beta}{1+\beta}} \Gamma_\beta dt. \quad (46)$$

Using equation (2) we get

$$\frac{d(j_x + ij_y)}{j_x + ij_y} = \frac{4\pi i G C_2}{c^2} (1+\beta)^{\frac{\beta}{1+\beta}} \kappa^{-\frac{1+2\beta}{2(1+\beta)}} \Gamma_\beta dt \quad (47)$$

and equation (11) for κ we get

$$\begin{aligned} \frac{d(j_x + ij_y)}{j_x + ij_y} = & -(-i)^{\frac{1}{2(1+\beta)}} \frac{2\pi (G^3 M)^{1/2} \Sigma_0}{c^2} R_0^{\frac{\beta}{2(1+\beta)}} 2^{\frac{1}{2(1+\beta)}} \\ & \times (1+\beta)^{\frac{\beta}{1+\beta}} \left(\frac{\omega_p}{\nu_{20}} \right)^{-\frac{1+2\beta}{2(1+\beta)}} \Gamma_\beta dt. \end{aligned} \quad (48)$$

Then using equations (2) and (3) we find

$$\begin{aligned} \frac{d(j_x + ij_y)}{j_x + ij_y} = & -(-i)^{\frac{1}{2(1+\beta)}} \frac{2\pi (G^3 M)^{1/2} \Sigma_0}{c^2} R_0^{\frac{\beta}{2(1+\beta)}} \\ & \times \left(\frac{1+\beta}{2} \right)^{\frac{\beta}{1+\beta}} \left(\frac{aG^2 M^2}{\nu_{20} c^3} \right)^{-\frac{1+2\beta}{2(1+\beta)}} \\ & \times \Gamma_\beta dt. \end{aligned} \quad (49)$$

We can rewrite equation (49) as

$$\frac{d(j_x + ij_y)}{j_x + ij_y} = -(-i)^{\frac{1}{2(1+\beta)}} \frac{dt}{T} \quad (50)$$

by setting

$$\begin{aligned} T^{-1} = & \frac{2\pi (G^3 M)^{1/2} \Sigma_0}{c^2} R_0^{\frac{\beta}{2(1+\beta)}} \left(\frac{1+\beta}{2} \right)^{\frac{\beta}{1+\beta}} \\ & \left(\frac{aG^2 M^2}{\nu_{20} c^3} \right)^{-\frac{1+2\beta}{2(1+\beta)}} \Gamma_\beta. \end{aligned} \quad (51)$$

We can then integrate to find

$$\begin{aligned} j_x + ij_y = & A \exp \left[-(-i)^{\frac{1}{2(1+\beta)}} \frac{t}{T} \right] \\ = & A \exp \left[-\cos \left(\frac{\pi}{4(1+\beta)} \right) \frac{t}{T} \right] \\ & \times \exp \left[i \sin \left(\frac{\pi}{4(1+\beta)} \right) \frac{t}{T} \right], \end{aligned} \quad (52)$$

where A is the value of $j_x + ij_y$ at $t = 0$. In Figure 4 we plot the evolution of j_y against j_x with $A = 1$ so $j_x = 1$ and $j_y = 0$ at $t = 0$. The points along the lines are at times $t = 1, 2, 3$ and $4T$.

4.1 Alignment Timescale

Thus the timescale for alignment of the black hole is

$$\begin{aligned} t_{\text{align}} = & \frac{T}{\cos \left(\frac{\pi}{4(1+\beta)} \right)} \\ = & \frac{c^2}{2\pi (G^3 M)^{1/2} \Sigma_0} R_0^{-\frac{\beta}{2(1+\beta)}} \left(\frac{2}{1+\beta} \right)^{\frac{\beta}{1+\beta}} \\ & \times \left(\frac{aG^2 M^2}{\nu_{20} c^3} \right)^{\frac{1+2\beta}{2(1+\beta)}} \frac{\Gamma \left(\frac{1}{2(1+\beta)} \right)}{\Gamma \left(\frac{1+2\beta}{2(1+\beta)} \right)} \\ & \times \frac{1}{\cos \left(\frac{\pi}{4(1+\beta)} \right)}. \end{aligned} \quad (53)$$

Putting $R_0 = R_{\text{warp}}$ we find

$$\begin{aligned} t_{\text{align}} = & \frac{c^2}{4\pi (G^3 M)^{1/2} \Sigma_0} R_{\text{warp}}^{1/2} (1+\beta)^{-\frac{\beta}{1+\beta}} \\ & \times \frac{\Gamma \left(\frac{1}{2(1+\beta)} \right)}{\Gamma \left(\frac{1+2\beta}{2(1+\beta)} \right) \cos \left(\frac{\pi}{4(1+\beta)} \right)}. \end{aligned} \quad (54)$$

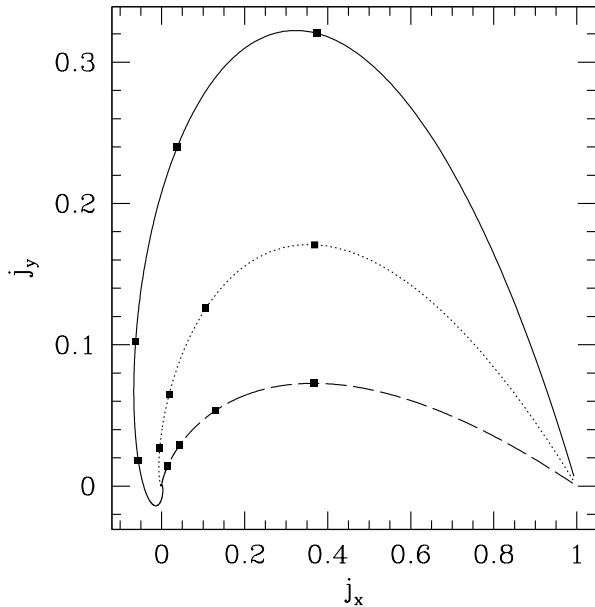


Figure 4. The angular momentum of the hole, j_y against j_x evolving in time. Initially $j_x = 1$ and $j_y = 0$. The points along the lines are at times $t = 1, 2, 3$ and $4T$.

If $\beta = 0$ then we get

$$t_{\text{align}}(0) = \frac{1}{\sqrt{2}\pi\Sigma_0} \left(\frac{acM}{\nu_{20}G} \right)^{\frac{1}{2}} \quad (55)$$

which agrees with Scheuer & Feiler (1996) who omitted a factor of $\sqrt{2}$.

We can write the timescale to align with β in terms of the timescale with $\beta = 0$ so that

$$\frac{t_{\text{align}}(\beta)}{t_{\text{align}}(0)} = \frac{(1+\beta)^{-\frac{\beta}{1+\beta}}}{\sqrt{2}} \frac{\Gamma\left(\frac{1}{2(1+\beta)}\right)}{\Gamma\left(\frac{1+2\beta}{2(1+\beta)}\right) \cos\left(\frac{\pi}{4(1+\beta)}\right)}. \quad (56)$$

In Figure 5 we plot this ratio as a function of β . Like Natarajan & Armitage (1999), we see that as β increases, the timescale of alignment increases, but only by just under a factor of 2 as β varies from 0 to 3.

4.2 Precession Timescale

The precession timescale is

$$\begin{aligned} t_{\text{prec}} &= \frac{T}{\sin\left(\frac{\pi}{4(1+\beta)}\right)} \\ &= \frac{\cos\left(\frac{\pi}{4(1+\beta)}\right)}{\sin\left(\frac{\pi}{4(1+\beta)}\right)} t_{\text{align}} \\ &= \cot\left(\frac{\pi}{4(1+\beta)}\right) t_{\text{align}}. \end{aligned} \quad (57)$$

Thus, as found by Scheuer & Feiler (1996), when $\beta = 0$ these two timescales are identical. In Figure 6 we plot the ratio of the precession timescale to alignment timescale against β . If $\beta = 0$ then the alignment and precession timescales are the same but if $\beta > 0$ then the precession timescale is longer

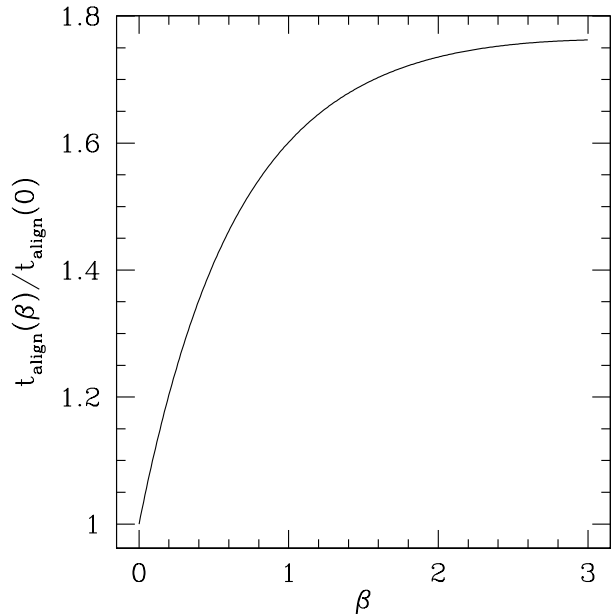


Figure 5. The alignment timescale against β normalised by the alignment timescale when $\beta = 0$.

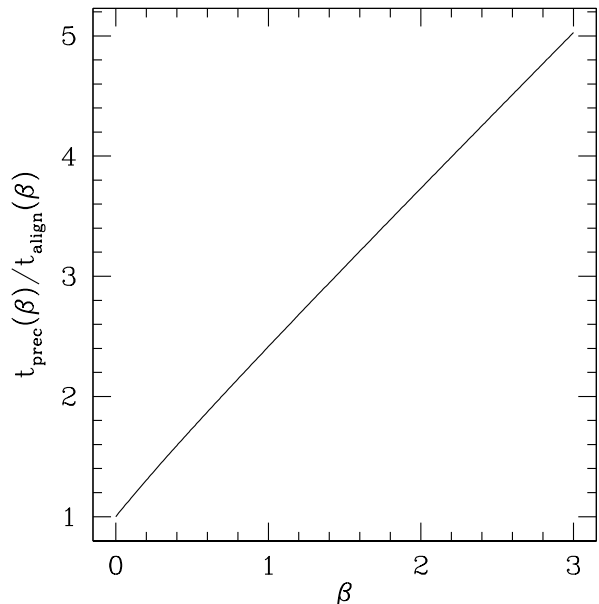


Figure 6. The precession timescale divided by the alignment timescale against β .

than the alignment timescale and increases with increasing β . This is also apparent from Figure 4.

5 TRUNCATION OF THE DISC

The results in the preceding Section were obtained under the assumption that the outer disc radius is infinite. We actually only require $R_{\text{out}} \gg R_{\text{warp}}$. However, this may not always be the case. For example in binary star systems the disc is

truncated at the tidal radius. We consider here the effects of truncating the disc at finite radius.

The mass of the disc in steady state is given by

$$\begin{aligned} M_{\text{disc}} &= 2\pi \int_{R_{\text{in}}}^{R_{\text{out}}} \Sigma R dR = 2\pi \Sigma_0 R_0^\beta \int_{R_{\text{in}}}^{R_{\text{out}}} R^{1-\beta} dR \\ &= \frac{2\pi \Sigma_0}{R_0^{-\beta} (2-\beta)} \left[R_{\text{out}}^{2-\beta} - R_{\text{in}}^{2-\beta} \right] \end{aligned} \quad (58)$$

if $\beta \neq 2$. If $\beta < 2$ then for finite mass R_{out} must be finite and if $\beta > 2$ then $R_{\text{in}} \neq 0$.

We consider the integral in equation (40). If we let $z = (1-i)y$ where y is real and

$$y = \frac{2}{(1+\beta)} \left(\frac{\omega_p}{\nu_{20}} \right)^{\frac{1}{2}} R_0^{\frac{\beta}{2}} R^{-\frac{1}{2}(1+\beta)} \quad (59)$$

then the integral becomes

$$Q = \int_{y_{\text{in}}}^{y_{\text{out}}} (1-i) K_{\frac{1}{2(1+\beta)}}((1-i)y) ((1-i)y)^{\frac{1+2\beta}{2(1+\beta)}} dy \quad (60)$$

We now define

$$P = \frac{\int_{y_{\text{out}}}^{\infty} (1-i) K_{\frac{1}{2(1+\beta)}}((1-i)y) ((1-i)y)^{\frac{1+2\beta}{2(1+\beta)}} dy}{\int_0^{\infty} (1-i) K_{\frac{1}{2(1+\beta)}}((1-i)y) ((1-i)y)^{\frac{1+2\beta}{2(1+\beta)}} dy} \quad (61)$$

where

$$y_{\text{out}} = \frac{2}{1+\beta} \left(\frac{\omega_p R_0^\beta}{\nu_{20}} \right)^{\frac{1}{2}} R_{\text{out}}^{-\frac{1}{2}(1+\beta)} \quad (62)$$

so that in units of $R_0 = R_{\text{warp}}$

$$y_{\text{out}} = \frac{\sqrt{2}}{1+\beta} \left(\frac{R_{\text{out}}}{R_{\text{warp}}} \right)^{-\frac{1}{2}(1+\beta)}. \quad (63)$$

Thus the quantity $P(y_{\text{out}})$ encapsulates the effect of truncating the disc at radius $R_{\text{out}}(y_{\text{out}})$. In Figure 7 we plot the effect of truncating the disc on the timescale for $\beta = 0, 3/4$ and 3 . We plot $|P|$ against $R_{\text{out}}/R_{\text{warp}}$. If $|P| = 1$ then truncating the disc at that radius has no effect on the timescale for alignment. We see that if β is higher, we can truncate the disc closer to the central black hole without affecting the timescales. If $\beta = 3$ we could truncate the disc at $R_{\text{out}} = 4R_{\text{warp}}$ whereas if $\beta = 0$ we cannot truncate the disc within $R_{\text{out}} \approx 10^4 R_{\text{warp}}$ and leave the timescales unchanged.

6 COUNTER ALIGNMENT

Scheuer & Feiler (1996) considered black holes almost anti-parallel to the discs. In this case we reverse the sign of ω_p and obtain

$$\kappa = \frac{2i\omega_p}{\nu_{20}} R_0^\beta \quad (64)$$

and hence equation (24) becomes

$$\begin{aligned} W &= \frac{2W_\infty}{\Gamma\left(\frac{1}{2(1+\beta)}\right)} \frac{(i)^{\frac{1}{4(1+\beta)}}}{(1+\beta)^{\frac{1}{2(1+\beta)}}} \left(\frac{R_{\text{warp}}}{R} \right)^{1/4} \\ &\times K_{\frac{1}{2(1+\beta)}} \left(\frac{\sqrt{2}}{1+\beta} (1+i) \left(\frac{R}{R_{\text{warp}}} \right)^{-\frac{1+\beta}{2}} \right) \end{aligned} \quad (65)$$

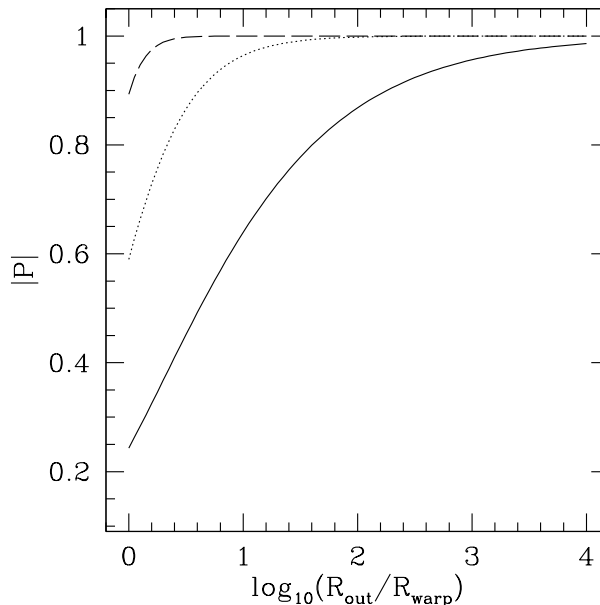


Figure 7. The modulus of P against $R_{\text{out}}/R_{\text{warp}}$. The solid line has $\beta = 0$, the dotted line has $\beta = 3/4$ and the dashed line has $\beta = 3$.

and equation (50) becomes

$$\frac{d(j_x + ij_y)}{j_x + ij_y} = i^{\frac{1}{2(1+\beta)}} \frac{dt}{T} \quad (66)$$

so that j_x and j_y increase exponentially and the disc realigns initially on the same timescale.

7 CONCLUSIONS

We have derived the steady state profile of a warped accretion disc in the case when the viscosity and the surface density vary as power laws in radial distance from the central black hole. We find that, compared to the analysis of Scheuer & Feiler (1996) where constant surface density was assumed, for more realistic situations in which the surface density is a decreasing function of radius, the timescale for alignment of a black hole with its accretion disc increases slightly while the timescale of precession is more greatly increased. For constant surface density Scheuer & Feiler (1996) found these two timescales to be the same. For more realistic density distributions we find that the black hole precesses at a much slower rate than the rate at which it aligns. If this process were responsible for changing the jet direction in an observed source then we would predict that there should be little evidence of precession.

ACKNOWLEDGEMENTS

We thank Phil Armitage and Priya Natarajan for helpful comments. RGM thanks STFC for a Studentship. CAT thanks Churchill College for a Fellowship.

REFERENCES

- Bardeen J. M., Petterson J. A., 1975, ApJ, 195, L65
 Gradshteyn I. S., Ryzhik I. M., 1980, Academic Press
 Greene J., Bailyn C. D., Orosz J. A., 2001, ApJ, 554, 1290
 Greenhill L. J., Kondratko P. T., Lovell J. E. J., Kuiper T. B., Moran J. M., Jauncey D. L., Baines G. P., 2003, ApJ, 582, L11
 Herrnstein J. R., Greenhill L. J., Moran J. M., 1996, ApJ, 468, L17
 Hjellming R. M., Rupen M. P., 1995, Nat, 375, 464
 King A. R., Lubow S. H., Ogilvie G. I., Pringle J. E., 2005, MNRAS, 363, 49
 Kinney A. L., Schmitt H. R., Clarke C. J., Pringle J. E., Ulvestad J. S., Antonucci R. R. J., 2000, ApJ, 537, 152
 Kumar S., Pringle J. E., 1985, MNRAS, 213, 435
 Lodato G., Pringle J. E., 2006, MNRAS, 368, 1196
 Lodato G., Pringle J. E., 2007, MNRAS, submitted
 Natarajan P., Armitage P. J., 1999, MNRAS, 309, 961
 Pringle J. E., 1981, ARA&A, 19, 137
 Pringle J. E., 1992, MNRAS, 258, 811
 Scheuer P. A. G., Feiler R., 1996, MNRAS, 282, 291
 Schmitt H. R., Pringle J. E., Clarke C. J., Kinney A. L., 2002, ApJ, 575, 150
 Watson G. N., 1966, 'A Treatise on the Theory of Bessel Functions', 2nd ed. Cambridge, England, CUP

APPENDIX 1

From tables of integrals (Gradshteyn & Ryzhik 1980) we find

$$\int_0^\infty K_c(z) z^d dz = 2^{d-1} \Gamma\left(\frac{1}{2}(1-c+d)\right) \times \Gamma\left(\frac{1}{2}(1+c+d)\right) \quad (67)$$

valid for $\Re(c-d) < 1$ and $\Re(c+d) > -1$. We need the integral over $(0, (1-i)\infty)$ along the contour C_0 in Figure 8. There are no singularities in $K_c(z)z^d$ other than a branch point at the origin when d is not an integer. We have

$$Q = \int_0^{(1-i)\infty} K_c(z) z^d dz = \int_0^\infty K_c(z) z^d dz + Q_2 + Q_3 \quad (68)$$

where Q_2 is the integral along contour C_2 over $z = Se^{i\theta}$ as $S \rightarrow \infty$ and Q_3 is the integral along contour C_3 over $z = \epsilon e^{i\theta}$ as $\epsilon \rightarrow 0$ with $-\pi/4 < \theta < 0$. We find

$$Q_2 = \lim_{S \rightarrow \infty} \int_0^{-\pi/4} i K_c(Se^{i\theta}) S^{d+1} e^{i\theta(d+1)} d\theta \quad (69)$$

so that

$$\begin{aligned} |Q_2| &\leq \lim_{S \rightarrow \infty} \int_0^{-\pi/4} |K_c(Se^{i\theta}) S^{d+1}| d\theta \\ &\sim \left(\frac{\pi}{2}\right)^{1/2} \lim_{S \rightarrow \infty} \left[S^{d+1/2} \int_0^{-\pi/4} e^{-S \cos \theta} d\theta \right] \\ &\rightarrow 0 \end{aligned} \quad (70)$$

as $S \rightarrow \infty$ if $\cos \theta \geq 0$ so that $-\pi/2 < \theta < \pi/2$. We have used the asymptotic expansion (Watson 1966)

$$K_c(z) \sim \left(\frac{\pi}{2z}\right)^{1/2} e^{-z} (1 + \dots), \quad (71)$$

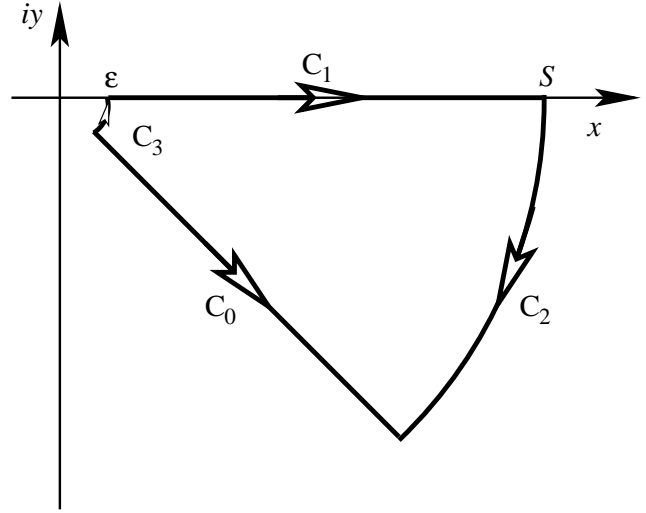


Figure 8. The complex contour of integration. The contour C_0 is the integral we need. We know the integral over C_1 .

as $z \rightarrow 0$. We have

$$Q_3 = \lim_{\epsilon \rightarrow 0} \int_{-\pi/4}^0 i K_c(\epsilon e^{i\theta}) \epsilon^{d+1} e^{i\theta(d+1)} d\theta \quad (72)$$

and using the approximation in equation (18) we find

$$\begin{aligned} |Q_3| &\leq \lim_{\epsilon \rightarrow 0} \left[\epsilon^{d+1} \int_{-\pi/4}^0 |K_c(\epsilon e^{i\theta})| d\theta \right] \\ &\sim \frac{\pi}{4} \frac{\Gamma(c)}{2^{1-c}} \epsilon^{d-c+1} \\ &\rightarrow 0 \end{aligned} \quad (73)$$

because $\Re(c-d) < 1$. Thus

$$Q = \int_0^{(1-i)\infty} K_c(z) z^d dz = \int_0^\infty K_c(z) z^d dz. \quad (74)$$